

Analyzing the Effects of Slope and Flow Rate on Fluid Dynamics with Cubic Obstacles in Open Channels

Thamir Mohammed Ahmed ^{2*} , Azeez Majeed Mohammed ¹, Nevin Celik ¹ , and Abdullah Hasan ² 

¹ Mechanical Engineering Department, Engineering Faculty, Firat University, Elazığ, Türkiye.

² Civil Engineering Department, Engineering Faculty, Tishk International University, Erbil, Iraq.

Article History

Received: 14.01.2025

Revised: 04.03.2025

Accepted: 25.03.2025

Published: 25.03.2025

Communicated by: Asst. Prof. Dr.

Abubakar M. Ashir

*Email address:

thamir.ahmed@tiu.edu.iq

*Corresponding Author



Copyright: © 2024 by the author. Licensee Tishk International University, Erbil, Iraq.

This article is an open-access article distributed under the terms and conditions of the Creative Commons Attribution License 4.0 (CC BY-4.0).

<https://creativecommons.org/licenses/by/4.0/>

Abstract: Abstract: This study investigates the impact of cubic obstacles on the velocity behavior of water flow in open channels under varying conditions. The cubic obstacles are designed to disrupt the smooth flow of water, inducing flow separation and reattachment, which in turn affects the velocity distribution and overall stability of the flow. Utilizing three different channel slopes ($S = 0^\circ$, 1.02° , and 1.4°) and three distinct flow rates ($Q = 0.0035 \text{ m}^3/\text{sec}$, $Q = 0.004 \text{ m}^3/\text{sec}$, and $Q = 0.0045 \text{ m}^3/\text{sec}$), the research focuses on the dynamics of flow separation and reattachment induced by the presence of these obstacles. The methodology involves both experimental works and computational fluid dynamics simulations to analyze the flow patterns, drag forces, and the resulting velocity profiles. Results reveal significant alterations in streamlines, with the cubic obstacles affecting not only the velocity distribution but also the overall stability of the flow. The findings highlight the critical role of slope and flow rate in influencing the interaction between fluid dynamics and channel geometry, providing insights for optimizing the design and functionality of open channels in urban drainage systems.

Keywords: Open Channel Flow; Cubic Obstacles; Flow Separation And Reattachment; Velocity Distribution; Drag Force; Channel Slope; Flow Rates Computational Fluid Dynamics.

1. Introduction

Open channels are an essential part of drainage systems, efficiently conveying stormwater runoff from urban areas to larger bodies of water such as rivers or lakes [1]. They are multi-purpose structures, varying in type and configuration, and serve as the final component of stormwater management. Beyond their primary function of conveying stormwater runoff, the design of open channels also affects stability, aesthetics, resource management, and public acceptance in urban environments [2]. Open channel flow occurs when a fluid, such as water, flows over a free surface exposed to the atmosphere, driven by gravitational forces. These flows are partially enclosed by rigid boundaries, such as canals or rivers, and are not subject to any gauge pressure at the surface [3], [4], and [5]. To facilitate flow, the bottom of the channel slopes, allowing gravity to move the water downward [6] and [7]. Channel design must take this into account while ensuring that the flow is stable and directed effectively.

Turbulence is common in open channel flows, especially in natural environments such as rivers, lakes, and streams. It is characterized by chaotic motions that promote the mixing and transfer of momentum and mass [8] and [9]. The interaction of environmental features, such as rocks or vegetation, with flowing water, can intensify turbulence, affecting local and global flow patterns [10]. The analysis of open channel flows includes key parameters such as channel geometry (slope, width, and roughness), fluid properties (viscosity and density), and flow characteristics (velocity and depth) [11] and [12].

Flow depth is critical because it determines both the energy and volume of the flow, making it essential for solving complex problems related to open-channel hydraulics. In addition, velocity varies across the depth and width of the channel, influenced by factors such as shape and surface roughness [13], and [14]. This diversity, combined with the need to manage frictional and energy losses, increases the complexity of the study and design of open channel systems.

This study investigates the impact of cubic obstacles on the velocity behavior of water flow in open channels under varying conditions. By examining three different channel slopes ($S = 0^\circ$, 1.02° , and 1.4°) and three distinct flow rates ($Q = 0.0035 \text{ m}^3/\text{sec}$, $Q = 0.004 \text{ m}^3/\text{sec}$, and $Q = 0.0045 \text{ m}^3/\text{sec}$), the manuscript aims to explore the dynamics of flow separation and reattachment induced by the presence of these obstacles. The role of cubic obstacles, which disrupt the smooth flow and alter velocity distribution, is critical in understanding the interaction between flow patterns, drag forces, and channel stability. The results provide valuable insights into how slope and flow rate influence the behavior of water flow and channel geometry. The ultimate goal is to optimize open channel design in urban drainage systems by improving stability and flow efficiency, which can be achieved through a better understanding of fluid dynamics in the presence of obstacles.

2. Methodology

The methodology of this study is based on both experimental and numerical methods to determine the flow behavior in a rectangular channel with cubic obstacles.

2.1 Experimental work

The rectangular channel, measuring 4 m in length, 30 cm in width, and 40 cm in depth, contains cubic obstacles of $2 \text{ cm} \times 2 \text{ cm} \times 2 \text{ cm}$ placed at three positions left, middle, and right, spaced 15 cm apart along a section spanning 150 cm to 275 cm (covering 31.25% of the total channel length). Despite the obstacles being 6.67% of the channel width, their height is 40% of the maximum flow depth (5 cm), making them significant in influencing velocity distribution, turbulence, and wake formation. Their relatively small size compared to the channel dimensions ensures minimal direct blockage, but their interaction with the shallow flow depth leads to pronounced vortex shedding, increased turbulence intensity, and variations in velocity recovery downstream. The flow behavior was investigated by measuring the velocity changes along the channel at various flow rates ($\dot{Q} = 0.0035 \text{ m}^3/\text{s}$, $0.004 \text{ m}^3/\text{s}$, and $0.0045 \text{ m}^3/\text{s}$) and slopes ($S = 0^\circ$, 1.02° , and 1.406°). Measurements were made at three points across each cross-section (left, middle, right) to evaluate how cubic obstacles affect flow patterns, including flow separation, re-adhesion, drag force, and sedimentation. Figure (1).

2.2 Numerical work

Numerical simulations were performed to complement the experimental data using computational fluid dynamics (CFD). The numerical model simulated the velocity distribution and flow characteristics around cubic obstacles, allowing for visualization of separation zones, vortex formation, and shear stress distribution. Results from the simulations were compared to experimental data to validate the flow patterns and analyze the effect of flow rate and slope on velocity profiles, turbulence, and drag forces. The flow behavior was modeled based on the principles of fluid dynamics, which are primarily governed by the Navier-Stokes equations for incompressible flow, which describe the motion of fluid materials. These two equations are the primary ones that govern the flow of water as a Newtonian fluid in numerical simulations are as follows,[5],[12], and [16]:

Continuity Equation (Conservation of Mass for Incompressible Flow): Since water is incompressible, the continuity equation simplifies to:

$$(1) \quad \nabla \cdot \mathbf{v} = 0$$

Where v is the velocity vector.

Navier-Stokes Equation (Conservation of Momentum): For a Newtonian fluid like water, the Navier-Stokes equation governs the momentum conservation, accounting for viscosity:

$$(2) \quad \rho(\partial v/\partial t + v \cdot \nabla v) = -\nabla p + \mu \nabla^2 v + f$$

Where ρ is the fluid density, kN/m^3 , p is the pressure, kPa , μ : is the dynamic viscosity of water, m^2/sec , and f represents external forces (e.g., gravity).

Both experimental and numerical data were used to explore how cubic obstacles alter flow dynamics, including drag force, turbulence, and flow separation.



Figure 1: Experimental setup of the open channel in the laboratory

3. Results and Discussion

The study examines the flow behavior in a rectangular channel (4 m long, 30 cm wide, and 40 cm deep) with cubic obstacles (2 cm 2 cm 2 cm) installed at three locations: left, middle, and right. These obstacles are spaced 15 cm apart, starting 150 cm from the channel's entrance and extending up to 275 cm. Velocity changes along the channel are measured at three points across each cross-section: left, middle, and right. In this study, three different channel slopes ($S=0^\circ, 1.02^\circ$, and 1.4°) and due to some limitations in the pump, three distinct flow rates ($\dot{Q} = 0.0035 \text{ m}^3/\text{s}$, $0.004 \text{ m}^3/\text{s}$, and $0.0045 \text{ m}^3/\text{s}$) are used. The aim is to understand how the orientation and shape of the obstacles affect the velocity distribution and how flow separation, re-adhesion, drag force, and sedimentation occur.

Flow characteristics at $\dot{Q} = 0.0035 \text{ m}^3/\text{s}$ and $S = 0^\circ$ (Figure 2): The velocity changes along the channel, with cubic obstacles under these conditions, show clear trends in both the experimental and numerical data. Flow around cubic obstacles produces noticeable, if less pronounced, turbulence compared to more complex shapes. As the flow approaches each obstacle, a decrease in velocity is observed due to the obstacle, creating a wake region downstream. These wakes consist of separation zones where the flow rejoins, creating a vortex. These vortices redistribute momentum and cause mixing in the flow, although the effect remains moderate due to the regular cubic shape. The presence of cubic obstacles also affects the distribution of shear stress on the channel surfaces and obstacles. Due to the sharp edges of the cubes, areas of high shear stress are observed at the points where the flow hits the obstacles, while there is less shear stress in the wake regions. The drag force on the obstacles is moderate due to their block-like structure, which is less streamlined compared to other shapes, but it still affects the overall flow dynamics, especially in terms of flow resistance and energy dissipation.

Flow characteristics at $\dot{Q} = 0.004 \text{ m}^3/\text{s}$ and $S = 0^\circ$ (Figure 3): As the flow rate increases, the general trends from the low flow rate remain the same, but the turbulence caused by the obstacles becomes more pronounced. The higher velocities ahead of the obstacles enhance the drag force and shear stress, especially at the surfaces of the obstacles. The higher flow rate amplifies the flow separation, resulting in a more pronounced vortex formation in the wake of each obstacle. The wake regions behind the cubes expand more downstream, with slower velocity recovery than in the low flow rate case. The stronger interaction between the flow and the obstacles causes more significant changes in the velocity distribution, increasing the shear stress on the channel bed and walls.

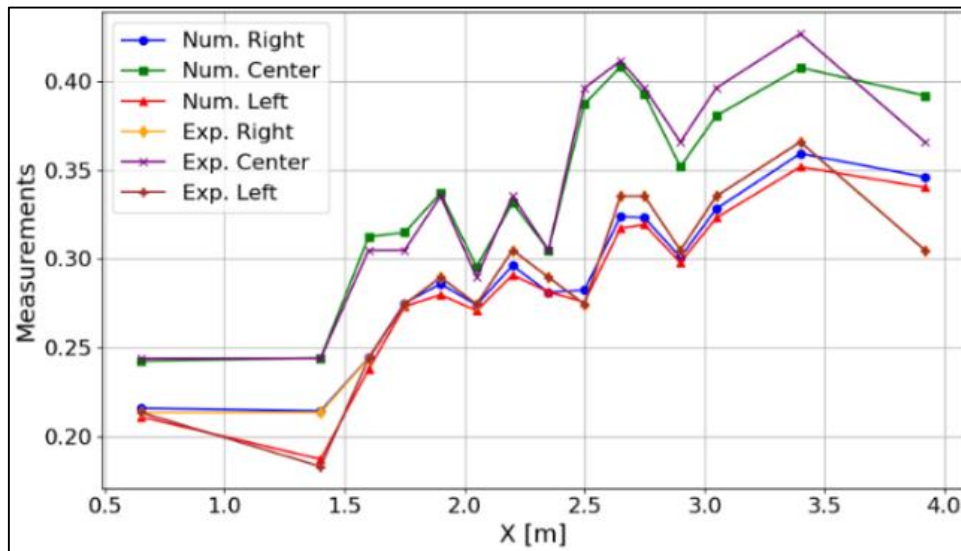


Figure 2: Velocity Variation for $Q = 0.0035 \text{ m}^3/\text{s}, S = 0^\circ$

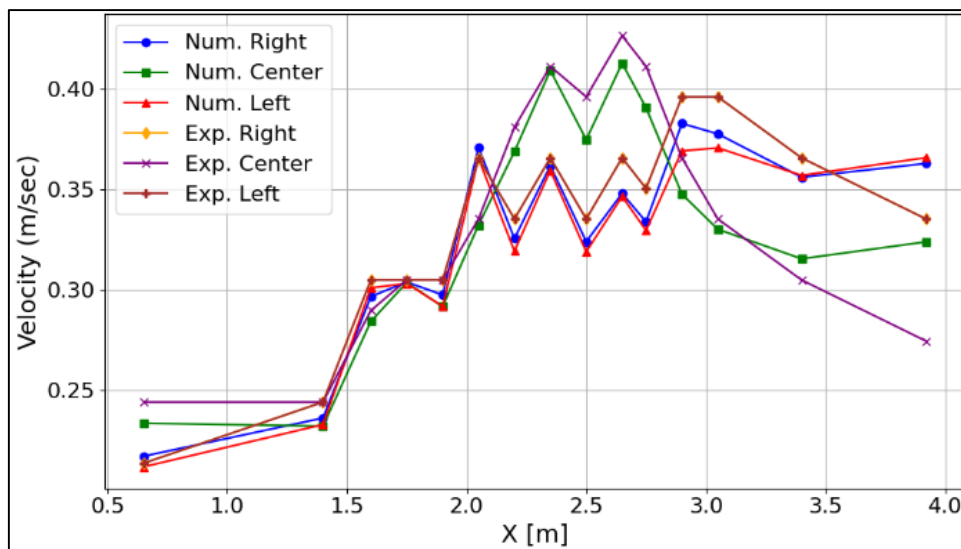
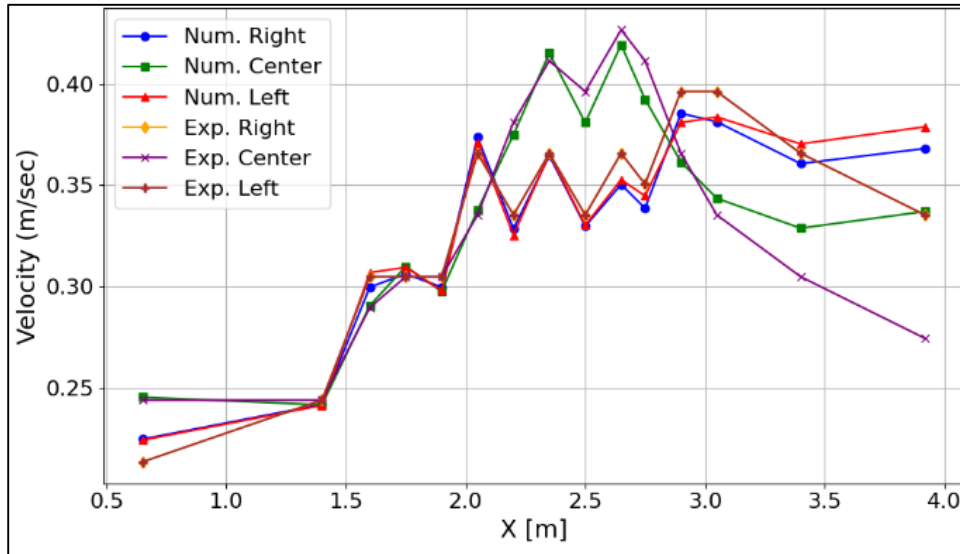
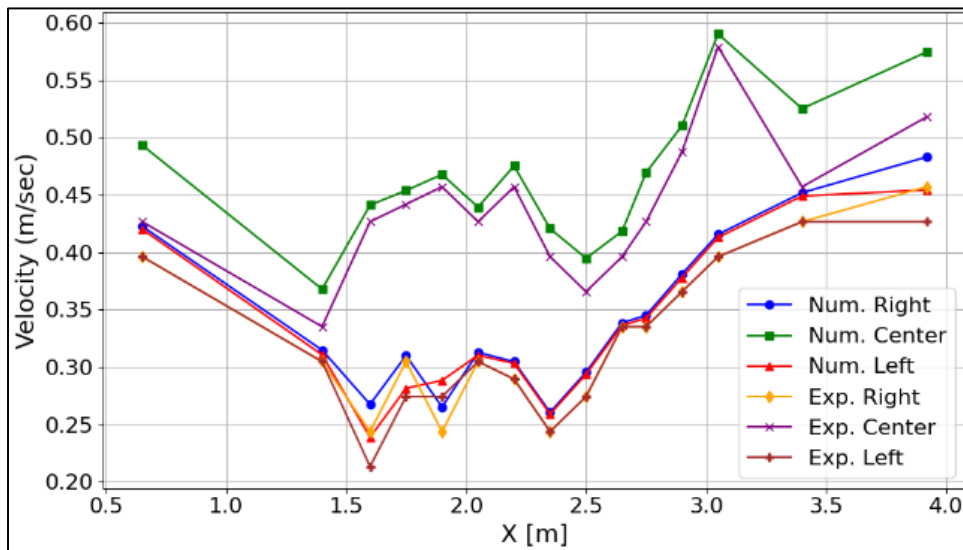


Figure 3: Velocity Variation for $Q = 0.004 \text{ m}^3/\text{s}, S = 0^\circ$

Flow characteristics at $\dot{Q} = 0.0045 \text{ m}^3/\text{s}$ and $S = 0^\circ$ (Figure 4): Under these conditions, the effects of the obstacles are intensified due to the increased flow velocity. The greater momentum of the flow leads to stronger separation and more defined vortices in the wake regions. Higher flow rates increase the drag force on the cubes and the associated shear stress on the surrounding surfaces. Recovery of the flow between obstacles is delayed, with lower velocities observed in the gaps between obstacles. The increased flow velocity also increases the overall turbulence in the system, leading to greater momentum redistribution and enhanced mixing.

Figure 4: Velocity Variation for $Q = 0.0045 \text{ m}^3/\text{s}, S = 0^\circ$ Figure 5: Velocity Variation for $Q = 0.0035 \text{ m}^3/\text{s}, S = 1.02^\circ$

Gravitational forces have a major impact on flow behavior at a flow rate of $Q=0.0035 \text{ m}^3/\text{s}$ and a slope of $S=1.02^\circ$ (Figure 5), speeding the water downstream. Because of the higher slope, the velocity profiles show more noticeable shifts, increasing before the obstacles and then sharply declining downstream as flow separation and greater eddies form. Increased turbulence and shear stress result from the flow and cubic barriers' increasingly intricate interaction. Additionally, the steeper slope increases drag forces on the obstructions, which alters flow dynamics and energy dissipation. The overlapping velocity curves indicate a comparatively uniform distribution, which may indicate fully formed flow, laminar conditions, or flow symmetry.

The validity of the results is further enhanced by the consistency of experimental and numerical results in stable zones. Depending on their configuration and the channel conditions, the cubic barriers interrupt the flow through acceleration, recirculation, and flow separation zones, which causes the velocity changes. They increase turbulence by creating eddies and vortices that lead to localized changes in velocity, especially around the margins of obstacles where flow separation and reattachment take place. Together, these events affect the channel's overall stability and energy distribution in addition to localized velocity anomalies.

Flow characteristics at $\dot{Q} = 0.004 \text{ m}^3/\text{s}$ and $S = 1.02^\circ$ (Figure 6): As flow rate and slope increase, the effects of cubic obstacles on flow become more pronounced. Higher velocity ahead of obstacles results in greater flow separation and larger vortex regions behind the cubes. Velocity profiles show large differences between the left, middle, and right sections, with the largest velocity decreases occurring in the regions immediately behind the obstacles. The interaction between flow and obstacles results in higher shear stresses on the channel bed and walls, contributing to enhanced sediment transport and potential erosion.

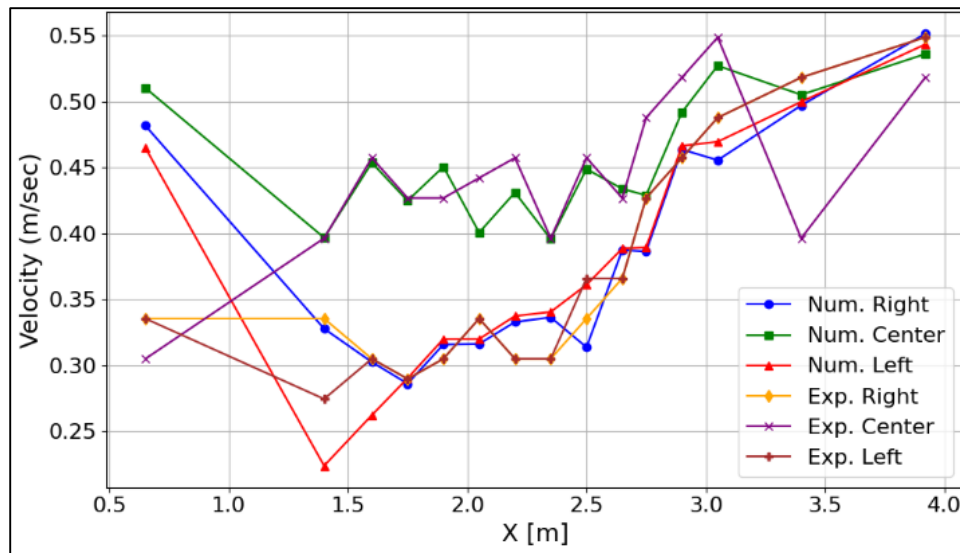


Figure 6: Velocity Variation for $Q = 0.004 \text{ m}^3/\text{s}$, $S = 1.02^\circ$

Flow characteristics at $\dot{Q} = 0.0045 \text{ m}^3/\text{s}$ and $S = 1.02^\circ$ (Figure 7): Higher flow rates amplify the separation regions behind the obstacles. As the flow moves over the cubes, pronounced separation and reconnection regions develop. This behavior leads to increased turbulence downstream, as well as increased drag and shear stresses on both the obstacles and the channel surfaces. The wake zones behind the obstacles become wider, with stronger vortices forming and greater momentum exchange.

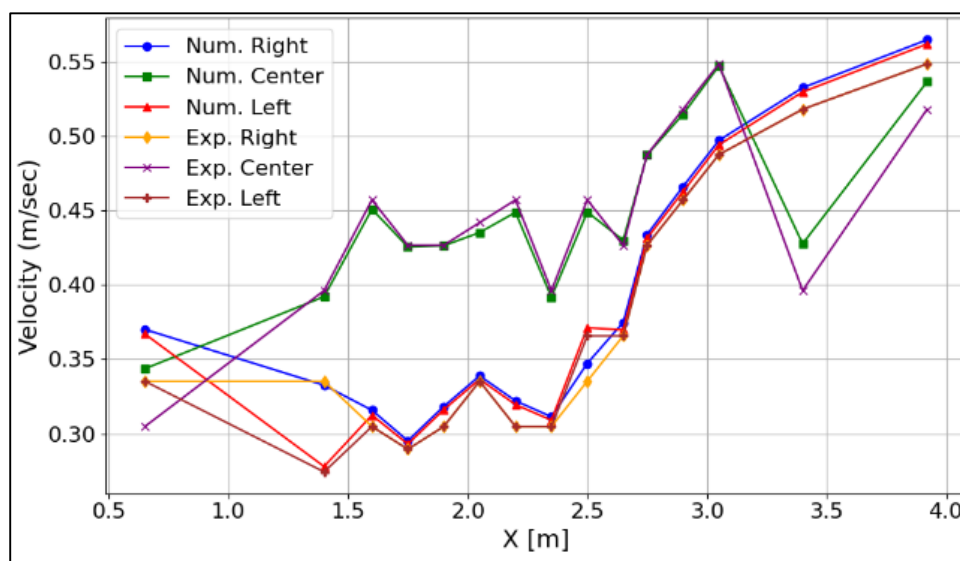


Figure 7: Velocity Variation for $Q = 0.0045 \text{ m}^3/\text{s}$, $S = 1.02^\circ$

Flow characteristics at $\dot{Q} = 0.0035 \text{ m}^3/\text{s}$ and $S = 1.406^\circ$ (Fig. 8): At this higher slope, gravity forces dominate the flow, causing more significant initial velocities ahead of the obstacles. The flow experiences significant separation as it passes over the cubes, resulting in larger vortices forming and stronger eddies forming. The drag forces on the obstacles are higher, and the shear stress on the channel bottom and walls increases accordingly.

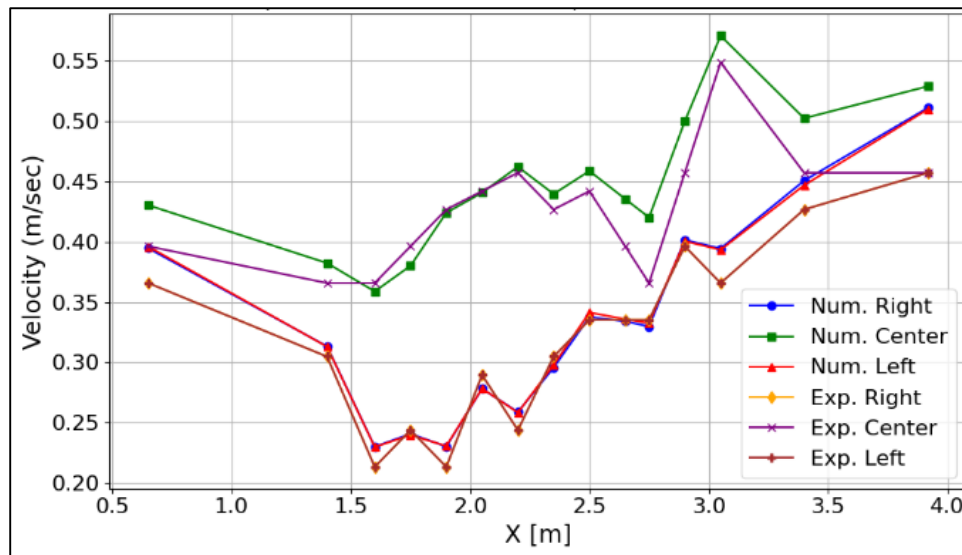


Figure 8: Velocity Variation for $Q = 0.0035 \text{ m}^3/\text{s}, S = 1.4^\circ$

Flow characteristics at $\dot{Q} = 0.004 \text{ m}^3/\text{s}$ and $S = 1.406^\circ$ (Fig. 9): For this case, the experimental and numerical results show similar trends. The flow velocity is highest in the center of the channel, where there is less of an obstacle. However, the flow slows down significantly near obstacles, especially in the right and left regions of the channel. The interactions between obstacles and flow lead to the formation of pronounced vortices and flow separation, which intensifies with increasing slope and flow rate.

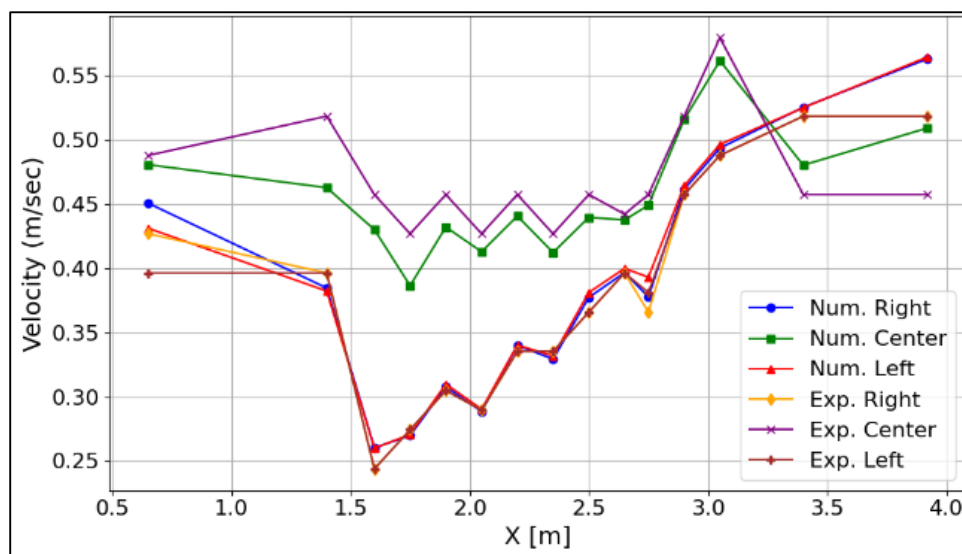


Figure 9: Velocity Variation for $Q = 0.004 \text{ m}^3/\text{s}, S = 1.4^\circ$

Velocity distribution in open-channel flow is significantly influenced by slope steepness, as it entails the balance between gravitational acceleration, flow resistance and turbulence. At a steeper slope

($S = 1.4^\circ$), and ($Q = 0.004 \text{ m}^3/\text{s}$), the velocity before encountering obstacles is notably higher due to the stronger gravitational component driving the flow. However, as the flow interacts with obstacles, significant velocity drops occur downstream due to increased energy dissipation from enhanced turbulence, vortex shedding, and flow separation. This is evident in the pronounced fluctuations observed in experimental and numerical velocity profiles, where sharp decelerations occur in the wake zones. In contrast, at lower slopes, the velocity profile exhibits a more gradual variation with fewer abrupt fluctuations. The reduced gravitational acceleration results in lower flow momentum, leading to weaker flow separation behind obstacles. Consequently, wake zones are less pronounced, and the velocity recovery downstream is more uniform. Additionally, the reduced shear stress at milder slopes limits the extent of turbulence-induced mixing, stabilizing velocity distributions along the channel. The comparison highlights that steeper slopes amplify velocity gradients and turbulence intensity due to stronger inertial effects and shear layers forming around obstructions. In contrast, lower slopes exhibit more laminar characteristics, with slower velocity recovery and reduced energy dissipation. These findings align with fundamental principles of open-channel hydraulics, where increasing slope enhances flow velocity but also intensifies turbulence, affecting overall flow stability and resistance mechanisms.

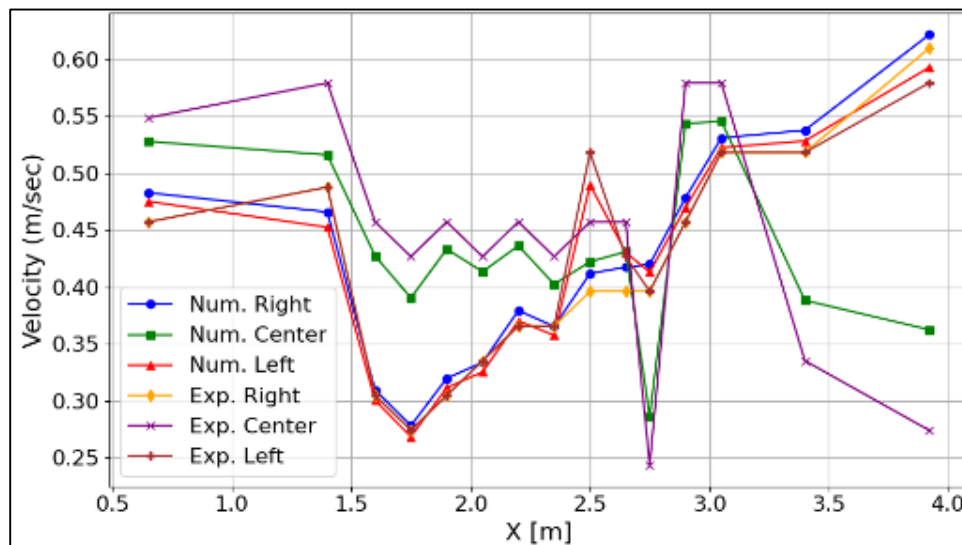


Figure 10: Velocity Variation for $Q = 0.0045 \text{ m}^3/\text{s}$, $S = 1.4^\circ$

Figure (11) shows the velocity profiles of cubic obstacles at a flow rate of $\dot{Q} = 0.0035 \text{ m}^3/\text{s}$ for slopes of 0° , 1.02° , and 1.406° . At a slope of 0° , the velocity profiles show a relatively uniform distribution before encountering the obstacles, with a moderate decrease in velocity downstream due to the small gravitational effect. The flow around the obstacles still creates separation zones and eddies, although their size and density remain limited due to the smaller flow rate and horizontal slope. For a slope of 1.02° , the velocity increases before the obstacles due to the steeper slope, resulting in a sharp decrease in velocity downstream as the flow separates and forms larger eddies behind the cubes. At the highest slope of 1.406° , the initial velocities before the obstacles are significantly higher due to the increased acceleration due to gravity, and the velocity decreases significantly after the obstacles due to the increased flow resistance and drag forces. The steeper slope causes a more pronounced effect on flow separation, vortex formation, and shear stress.

At increasing flow rate $\dot{Q} = 0.004 \text{ m}^3/\text{s}$, Figure (12) depicts the velocity patterns for slopes of 0° , 1.02° , and 1.406° . At 0° slope, the velocity distribution remains uniform before encountering obstacles, with a more significant decrease in velocity downstream than in the low flow rate case. The increase in flow

rate leads to more pronounced flow resistance and drag forces, causing stronger separation zones behind the cubes. For a slope of 1.02° , the velocity ahead of the obstacles increases significantly due to both the steeper slope and the higher flow rate. As a result, the flow separates more clearly behind the obstacles, creating larger vortices. At the steepest slope of 1.406° , the initial velocities are much higher, and flow separation behind the cubes becomes more significant. The combined effects of slope and flow rate create more significant flow disturbances, including stronger vortex formation, increased shear stress, and more pronounced drag forces.

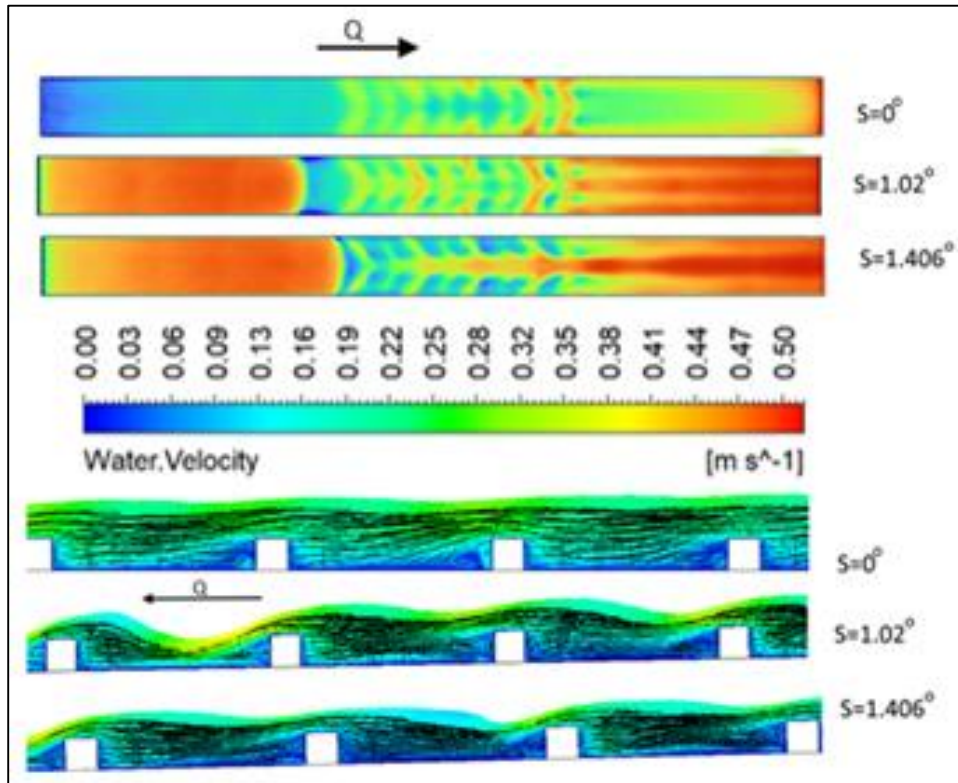


Figure 11: Numerical variation of velocity contours for cubic obstacle $Q = 0.0035 \text{ m}^3/\text{s}$.

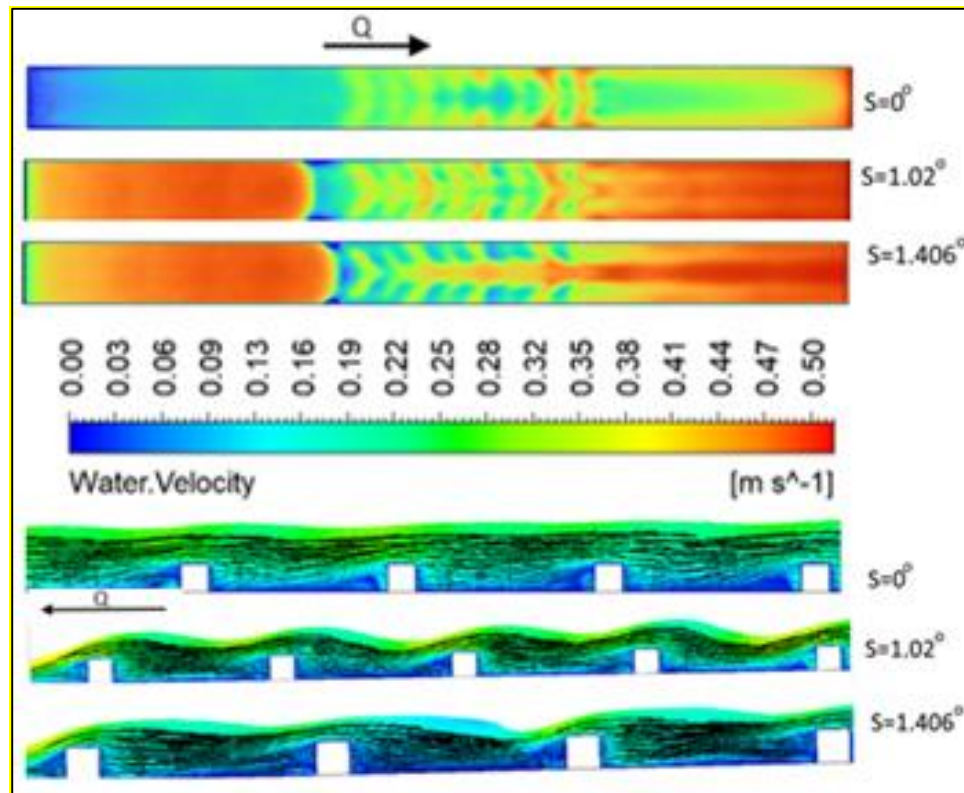


Figure 12: Numerical variation of velocity contours for cubic obstacle $Q = 0.004 \text{ m}^3/\text{s}$.

Flow characteristics for $\dot{Q} = 0.0045 \text{ m}^3/\text{s}$ and variable slopes (Figure 13): When the flow rate is increased to $\dot{Q} = 0.0045 \text{ m}^3/\text{s}$, Figures 3.45 and 3.46 show the velocity profiles for slopes of 0° , 1.02° , and 1.406° . At a slope of 0° , the velocity increases uniformly along the channel, but the presence of obstacles still causes a significant decrease in velocity downstream due to increased flow resistance. The larger flow rate promotes flow separation and vortex formation, with wake zones behind obstacles extending downstream. For a slope of 1.02° , the velocity increases more sharply before the obstacles due to the steeper slope and higher flow rate. After passing the obstacles, the velocity drops significantly, creating pronounced separation zones and vortices behind the cubes. At the steepest slope of 1.406° , the initial velocities are the highest, with flow rate and slope combining to create large drag forces and increased shear stress. Flow separation is more pronounced, and the wake zones behind the obstacles exhibit stronger vortex formation and turbulent flow behavior.

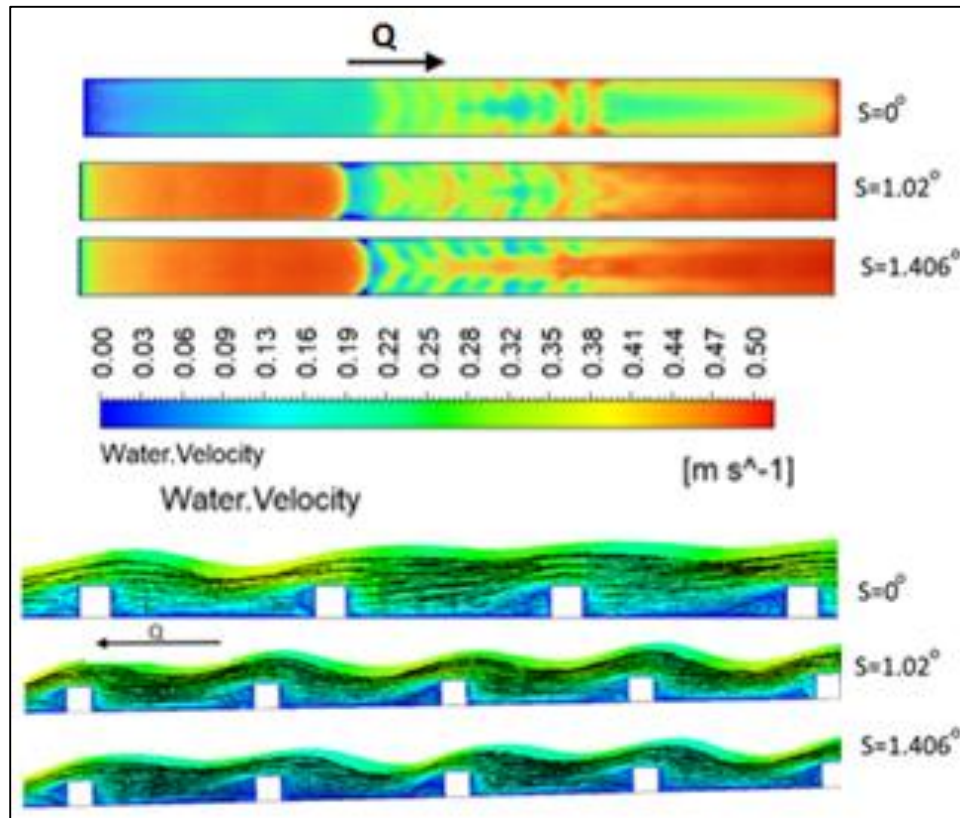


Figure 13: Numerical variation of velocity contours for cubic obstacle $Q = 0.0045 \text{ m}^3/\text{s}$.

4. Conclusions

The main conclusions of the study on the flow behavior in a rectangular channel with cubic obstacles can be summarized as follows:

1. Obstacle shape and orientation: Cubic obstructions cause turbulence and flow separation, with sharp edges leading to high shear stress. Wake zones have less shear, and vortex formation is less intense than complex shapes.
2. Flow rate effect: At flow rates of $0.0045 \text{ m}^3/\text{s}$, turbulence and drag increase. Velocity decreases significantly downstream, widening wake zones and promoting vortex formation, which increases shear stress.
3. Channel slope effect: Increasing slopes (0° , 1.02° , 1.406°) increase turbulence and velocity fluctuations. Steeper slopes cause rapid velocity drops, larger vortices, and greater flow separation.
4. Gravity and slope effects: At a flow rate of $0.0035 \text{ m}^3/\text{s}$ and a slope of 1.02° , gravity accelerates the flow ahead of obstructions, causing velocity spikes and sharp drops. Increased drag promotes turbulence, shear stress, and energy dissipation.
5. Flow separation and turbulence: Obstructions accelerate the flow, creating recirculation and separation zones, increasing turbulence, and changing velocity patterns, especially in wake zones.
6. Flow rate and slope on turbulence: Higher flow rates and slopes amplify separation, enlarge eddies, and increase shear stress, which enhances sediment transport and erosion.
7. High flow rate dynamics: At a flow rate of $0.0045 \text{ m}^3/\text{s}$, wake zones expand, eddies strengthen, and drag and shear stress on obstructions and channel surfaces increase.
8. At a slope of 1.406° , gravity, and higher flow rates produce higher initial velocities, which increase separation, eddy formation, turbulence, and energy dissipation.

9. Velocity distribution and flow interaction: Steeper slopes and higher flow rates cause sharper velocity drops after obstructions, and wake zones expand due to increased drag and turbulence.
10. Flow characteristics across slopes:
 - $S = 0^\circ$: uniform velocity, moderate downstream decline.
 - $S = 1.02^\circ$: acceleration ahead of obstacles, sharp velocity decrease, stronger wake zones.
 - $S = 1.406^\circ$: highest initial velocity, intense separation, larger eddies, and turbulence.
11. Flow rate vs. shear stress: Increasing flow rates from $0.0035 \text{ m}^3/\text{s}$ to $0.004 \text{ m}^3/\text{s}$ amplifies turbulence, shear stress, and expansion of the wake zone, which compresses the channel bottom and walls.
12. Slope and flow rate on stability: Higher flow rates and slopes intensify turbulence and eddy formation, which destabilizes the flow. Lower slopes exhibit smoother velocity changes, while steeper slopes amplify turbulence.

References

- [1] Moglen GE. Fundamentals of open channel flow. CRC Press; 2022 Dec 30. <https://doi.org/10.1201/b18359>
- [2] Deng J, Yin H, Kong F, Chen J, Dronova I, Pu Y. Determination of runoff response to variation in overland flow area by flow routes using UAV imagery. Journal of Environmental Management. 2020 Jul 1;265:109868. <https://doi.org/10.1016/j.jenvman.2019.109868>
- [3] Alam MS, Khan MA. MHD effects on mixed convection flow through a diverging channel with circular obstacle. Procedia Engineering. 2014 Jan 1;90:403-10. <https://doi.org/10.1016/j.proeng.2014.11.869>
- [4] Chanson H. Hydraulics of stepped chutes and spillways. CRC Press; 2002. <https://doi.org/10.1115/1.1523365>
- [5] Subramanya K. Flow in open channels. In Vascular (Issue January 2010). (2009).
- [6] Chalgeri VS, Jeong JH. Flow regime identification and classification based on void fraction and differential pressure of vertical two-phase flow in rectangular channel. International Journal of Heat and Mass Transfer. 2019 Apr 1;132:802-16. <https://doi.org/10.1016/j.ijheatmasstransfer.2018.12.015>
- [7] Sturm TW. Open channel hydraulics. New York: McGraw-Hill; 2001 Feb.
- [8] Chaudhry MH. Open-channel flow. New York: Springer; 2008 Apr.
- [9] Cant S. SB Pope, Turbulent Flows, Cambridge University Press, Cambridge, UK, 2000, 771 pp. Combustion and Flame. 2001;125(4):1361-2.
- [10] Zhou J. Physics of environmental flows interacting with obstacles. Department of Civil and Environmental Engineering, Doctor of, 2017. pp.167.
- [11] Natasha G, Noviantri V. Saint-venant model analysis of trapezoidal open channel water flow using finite difference method. Procedia Computer Science. 2019 Jan 1;157:6-15. <https://doi.org/10.1016/j.procs.2019.08.135>
- [12] Gond L, Perret G, Mignot E, Riviere N. Analytical prediction of the hydraulic jump detachment length in front of mounted obstacles in supercritical open-channel flows. Physics of Fluids. 2019 Apr 1;31(4). <https://doi.org/10.1063/1.5085744>
- [13] Ahmed S, Hossain A, Hossain MZ, Molla MM. Forced convection of non-Newtonian nanofluid in a sinusoidal wavy channel with response surface analysis and sensitivity test. Results in Engineering. 2023 Sep 1;19:101360. <https://doi.org/10.1016/j.rineng.2023.101360>
- [14] Tsynaeva A, Nikitin M. Numerical modeling of rectangular channel with shallow dumbbell dimples based Code Saturne. Proceedings of the Institute for System Programming of the RAS (Proceedings of ISP RAS). 2016;28(1):185-96. [https://doi.org/10.15514/ISPRAS-2016-28\(1\)-10](https://doi.org/10.15514/ISPRAS-2016-28(1)-10)